RSC Advances

ROYAL SOCIETY OF CHEMISTRY

www.rsc.org/advances

Journal Name

ARTICLE

Preparation of LiBOB via rheological phase method and its application to mitigate voltage fade of $Li_{1.16}[Mn_{0.75}Ni_{0.25}]_{0.84}O_2$ cathode

Received 00th January 20xx,
Accepted 00th January 20xx

DOI: 10.1039/x0xx00000x

www.rsc.org/

Fang Lian,[a]*, Yang Li,[a] Yi He,[a] Hongyan Guan,[a] Kun Yan,[a] Weihua Qiu,[a] Kuo-Chih Chou,[a] Peter Axmann[b] and Magret Wohlfahrt-Mehrens[b]

Lithium bis(oxalato)borate (LiBOB) were synthesized via a novel rheological phase reaction method without any recrystallization procedure. The purity of the as-obtained LiBOB has been identified in comparison with the commercial sample and our sample prepared from solid-state reaction method. The results of XRD, ICP, and ^{11}B NMR demonstrate that high pure LiBOB has been synthesized via rheological phase reaction method with significantly simplified synthetic process. Moreover, LiBOB sample has been investigated as electrolyte additive to improve the electrochemical performances of high-energy lithium-rich layered oxide. The cycling performances imply that 0.03M and 0.05M LiBOB additive can mitigate discharge voltage fade and enhance the cycle stability of $Li_{1.16}[Mn_{0.75}Ni_{0.25}]_{0.84}O_2$ material. The CV, EIS and XPS data indicate that LiBOB oxidizes at ~4.3 V (vs. Li/Li^+) on the cathode surface during the first charge to form a specific SEI layer with larger amount of organic species and fairly less content of LiF, which decreases the interfacial polarization and protects the active material from surface degradation, thereby mitigates the voltage-fade of Li-rich cathode.

1. Introduction

The electrolyte compositions (lithium hexafluorophosphate $LiPF_6$ and carbonate mixtures) have remained largely unchanged since the first lithium ion batteries were commercialized.[1] However, chemical and thermal instabilities of $LiPF_6$ restrict the application of lithium ion batteries especially in hybrid and electric vehicles, which generally require a service life of 10 years or longer under sustained electrochemical cycling[2, 3]. Even at room temperature $LiPF_6$ decomposes, resulting in the formation of solid deposition LiF and the strong Lewis acid PF_5, and the latter is reactive with organic solvents in the electrolytes. Both $LiPF_6$ and PF_5 will hydrolyze to form HF when trace amount of moisture exists.[4, 5] To solve the above issues, lithium bis(oxalato)borate (LiBOB) was first proposed as a promising candidate for $LiPF_6$ because of its advantages such as wide electrochemical window, high thermal stability, fluorine free in the structure, ability to passivate aluminum current collector, and ability to form a stable solid-electrolyte interface (SEI) at the surface of graphitic anode even in pure propylene carbonate (PC) solvent.[6, 7]

Angell and co-workers[8-10] synthesized LiBOB using lithium tetramethanolatoborate $LiB(OCH_3)_4$ and di(trimethylsilyl) oxalate $(CH_3)_3SiOOCCOOSi(CH_3)_3$ in anhydrous acetonitrile (AN). And then LiBOB was recrystallized from boiling AN/toluene (1:1 mixture), cooled to -20°C to obtain pure product. As reported, the common method for preparing LiBOB is based on organic solution reactions including the procedures such as dissolution, reflux, evaporation, etc., which are difficult to perform and commercialize. Our group employed the solid-state reaction to successfully synthesize LiBOB by heating the mixtures of oxalic acid dihydrate, lithium hydroxide and boric acid at 240°C for 6 hours in an open system, which is a simple, feasible and more environmentally friendly method.[11] However, the product obtained from the solid state reaction method contains impurities due to the open system and high heating temperature, which requires subsequent rigorous recrystallization to improve its purity. In the research of advance solutions to it, we propose a novel rheological phase reaction method to synthesize pure LiBOB without further recrystallization procedure for purification. The reaction occurs in a closed system at a lower heating temperature, while crystalline water and the water generated during the reaction process act as the solvent, preventing the introduction of impurities from additional reagent.

Nevertheless, the shortcomings of LiBOB have been exposed with researches going on: low solubility and conductivity when used with typical solvent systems, which renders the electrolyte system with poor rate capability and low-temperature performance.[12] Therefore, research interests have been transferred to focus on the application of LiBOB as functional electrolyte additive.[13-15] The high-energy lithium-

[a] School of Materials Science and Engineering, University of Science and Technology Beijing, Xueyuan Road, Haidian District, 100083 Beijing, P.R. China. E-mail: lianfang@mater.ustb.edu.cn
[b] Centre of Solar Energy and Hydrogen Research (ZSW) Baden-Württemberg, Helmholtzstr. 8, Ulm, 89081 Germany.

rich cathode $Li_{1+x}[Ni_yMn_{1-y}]_{1-x}O_2$ is believed to be a promising next generation cathode material due to its high specific capacity (>250 mAh/g) with larger charging voltages (>4.5 V vs. Li/Li^+).[16] As known, its problem on voltage- and capacity-fade during cycling still remains unsolved and limits the large-scale application. The aggressive oxidization and irreversible decompose of the commercial liquid electrolyte 1M $LiPF_6$ in EC/DMC at high cut-off voltage, moreover oxygen evolved from the activation of Li_2MnO_3 during the charge could induce or accelerate the deterioration of the high-energy cathode/electrolyte interface. The formation of a SEI layer with low conductivity and the attack of acidic species, such as HF, are believed to be the main reason for the deteriorated electrochemical performance of the Li-rich material during cycling. The application of SEI film-formation additive can effectively stabilize cathode/electrolyte interface and improve the performance of the cathodes.[15] For example, our previous work confirmed that fluoroethylene carbonate (FEC) could improve the electrochemical performances of the lithium-rich cathode $Li_{1.16}[Mn_{0.75}Ni_{0.25}]_{0.84}O_2$.[17] Choi *et al* reported that cycling stability of lithium-rich cathode $Li_{1.17}Ni_{0.17}Mn_{0.5}Co_{0.17}O_2$ could be enhanced by LiBOB additive which attributed to the LiBOB-derived protective layer on the cathode surface.[18] However, the impact of LiBOB additive on the discharge voltage fade of Li-rich cathode $Li_{1+x}[Ni_yMn_{1-y}]_{1-x}O_2$ has still been significantly less investigated to our knowledge.

In our work, LiBOB sample obtained via rheological phase reaction method (r-LiBOB) was evaluated by comparing with the commercial sample (c-LiBOB, *Chemtall*) and the one prepared from solid-state reaction method (s-LiBOB). As an additive of the state-of-the-art $LiPF_6$-based electrolyte, r-LiBOB was applied in lithium-rich cathode $Li_{1.16}[Mn_{0.75}Ni_{0.25}]_{0.84}O_2$ system to investigate the effect of LiBOB on its electrochemical performances, especially the discharge voltage fade issue.

2. Experimental

2.1 Synthesis of high-pure LiBOB

LiBOB was prepared via the novel rheological phase reaction method shown in Scheme 1 using the raw materials oxalic acid dihydrate $H_2C_2O_4{\cdot}2H_2O$ (≥ 99.5%), lithium hydroxide monohydrate $LiOH{\cdot}H_2O$ (≥ 96%) and boric acid H_3BO_3 (≥ 99.5%) with a mole ratio of 2:1:1. In detail, 12.6 g of $H_2C_2O_4{\cdot}2H_2O$ and 2.1 g of $LiOH{\cdot}H_2O$ were mechanically mixed in a stirrer for 5 minutes; then, 3.1 g of H_3BO_3 was added and stirred for another 5 minutes. The mixture was transferred into a sealed reactor and placed in a thermautostat at 110 °C for 6 hours. The gas generated during the heating process was released through the valve when the pressure in the sealed reactor exceeded 0.05 MPa. After 6 hours, the reaction system was cooled quickly in air, and then the coarse LiBOB precipitate was ground to a fine powder. The resulting samples were sequentially treated by microwave drying for 4 minutes at 70 °C, then by vacuum drying at room temperature for 5 hours to remove the residual adsorbed water, and finally by vacuum tube drying at 130 °C for 48 hours to eliminate the crystalline water. The reaction for the synthesis of r-LiBOB is shown in Equation 1.

$$2H_2C_2O_4{\cdot}2H_2O + LiOH{\cdot}H_2O + H_3BO_3 \rightarrow LiBOB + 9H_2O \quad (1)$$

The LiBOB sample (denoted as coarse-s-LiBOB) was also synthesized via solid-state reaction method on the basis of our previous work[11] according to Equation 1, which was purified by further recrystallization to obtain the pure sample (denoted as s-LiBOB).

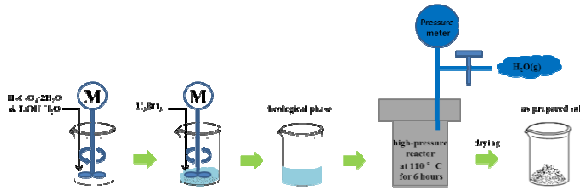

Scheme 1. The schematic diagram for the synthetic process of rheological phase reaction method

2.2 Cell preparation

The active material $Li_{1.16}[Mn_{0.75}Ni_{0.25}]_{0.84}O_2$ was prepared through a co-precipitation process using $LiOH{\cdot}H_2O$, $Ni(NO_3)_2{\cdot}6H_2O$ (all are 99.9% in purity) and $Mn(NO_3)_2$ (50% aqueous solution) as raw materials.[16] The mixed aqueous solution of 2.0 M transition metal nitrate and 2.0 M Na_2CO_3 solution were simultaneous added dropwise by peristaltic pump into a reactor, in which distilled water was under vigorous stirring. The resulting precipitates were filtered and washed three times to remove residual Na^+, and then dried under nitrogen at 120 °C for 24 hours. The as-obtained precursor was subsequently mixed with $LiOH{\cdot}H_2O$ using mortar and pestle. The mixture was sintered at 850 °C for 12 hours in muffle furnace under air.

The cathode was prepared from 85 wt.% active material $Li_{1.16}[Mn_{0.75}Ni_{0.25}]_{0.84}O_2$, 10 wt.% carbon black and 5 wt.% polyvinylidene difluoride (PVDF) dissolved in N-methyl-2-pyrrolidone (NMP). The slurry was coated on Al foil, and then heated at 120 °C in vacuum for 24 hours. Coin cells (2032) were fabricated in a dry argon filled glove box (*MBraun*) with metallic lithium and porous polypropylene films as anode and separator, respectively. Four electrolyte samples were involved herein: pristine 1M $LiPF_6$ in EC/ DMC/ DEC (1:1:1 in volume) electrolyte and the ones with various LiBOB contents (0.01M, 0.03M and 0.05M) in the pristine solution.

2.3 Measurements

The r-LiBOB, s-LiBOB, and c-LiBOB samples were analyzed by XRD, ICP, and ^{11}B NMR spectroscopy to identify the purity. XRD measurements of powder samples were performed on a XD2618N X-ray diffraction analyzer (*Japan*) at room temperature. ICP tests were measured by a Vista-MPX CCD inductive coupled plasma emission spectrometer (*United States*). ^{11}B NMR spectra were acquired using a Bruker AV600 nuclear magnetic resonance instrument (*Germany*) with a mixture solution of propylene carbonate (PC): ethylene carbonate (EC): dimethyl carbonate (DMC): γ-butyrolactone (GBL) (1:1:1:1, in volume) as solvent.

$Li/Li_{1.16}[Mn_{0.75}Ni_{0.25}]_{0.84}O_2$ cells with different electrolytes were cycled between 2.5V and 4.7V at a constant current density of 100mA/g (0.5C) using Land CT 2001 battery test system (*China*) at 25°C. Cyclic voltammetry (CV) and electrochemical impedance spectroscopy (EIS) were carried out on the Princeton VersaSTAT3 electrochemical work station (*United States*). CVs were performed with sweep rate of 0.1mV/s between 2.0V and 4.8V at 25°C using three-electrode cells (working electrode: $Li_{1.16}[Mn_{0.75}Ni_{0.25}]_{0.84}O_2$ cathode (Φ=1.6mm), counter electrode and reference electrode: Li foil). EIS were investigated at charged state of 4.0V at the 15th, 30th, 50th, and 100th cycles at frequency ranging from 100kHz to 0.01Hz under amplitude of 5mV, and the obtained impedance spectra were fitted by Zview program. The discharged $Li_{1.16}[Mn_{0.75}Ni_{0.25}]_{0.84}O_2$ electrodes were disassembled from the cells and then washed by DMC solvent to remove the residual electrolyte, finally dried under vacuum. The surface chemical components of the cycled electrodes were analyzed by Kratos AXIS Ultra DLD X-ray photoelectron spectroscopy (XPS) instrument (*Japan*) with Al Kα line as an X-ray source.

3. Results and discussion

3.1 Characterization of LiBOB samples

XRD patterns of r-LiBOB, s-LiBOB (also including the sample before purification, coarse-s-LiBOB) and c-LiBOB are compared in Fig. 1. The r-LiBOB sample shows similar diffraction pattern with the c-LiBOB and s-LiBOB. All the peaks of r-LiBOB sample can be indexed based on an orthorhombic structure (space group: Pnma, No. 62).[19] Besides, the main diffraction peaks intensities of r-LiBOB sample are stronger, indicating a higher degree of crystallization for the as-synthesized r-LiBOB salt. As shown in Fig. 1b, several impurity peaks are observed in the XRD pattern for the coarse-s-LiBOB sample:[20] peak at 11.25° associated with crystalline water; peaks at 20.08° and 28.01° related to HBO_2 (JCPDS card no. 22-1109), which is a product of H_3BO_3 decomposition; peak at 22.27° and 29.69° indexed to $Li_2C_2O_4$ (JCPDS card no. 24-0646), which is a side product of the reaction between $H_2C_2O_4{\cdot}2H_2O$ and $LiOH{\cdot}H_2O$. The s-LiBOB with high purity (Fig. 1c) was acquired after the removal of the impurities by recrystallization. Excitingly, these impurity peaks cannot be observed in the patterns of the r-LiBOB sample obtained via the rheological phase reaction method without any further purification.

Elemental analysis (ICP) results show that the r-LiBOB sample contains Li at 3.79 mass % (3.58% in theory), B at 5.70 mass % (5.58% in theory), and C_2O_4 at 90.51 mass % (90.84% in theory). It can be calculated that the atom ratio of Li to B to C_2O_4 was 1.04:1: 1.91, which was very close to the theoretical value of 1:1:2.

The LiBOB samples were further studied using ^{11}B NMR to compare their purity, as shown in Fig. 2. The ^{11}B spectrum for each sample (r-LiBOB, s-LiBOB and c-LiBOB) shows analogous features, corresponding to a chemical shift of ~7.6 ppm, which is the only contribution from BOB anion. The chemical shift of 7.677 ppm for the r-LiBOB sample is very close to the ^{11}B shift near 7.70 ppm of LiBOB using tetrahydrofuran (THF) solvent as reported earlier in the literature,[21] which is contributed to the introduction of different solvents for the test LiBOB samples. Therefore, LiBOB sample obtained using the rheological phase method possesses high purity and well meets the requirement of electrolyte for lithium ion batteries.

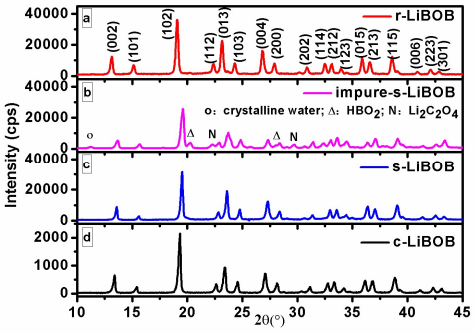

Fig. 1.XRD patterns of LiBOB samples: (a) r-LiBOB, (b) impure-s-LiBOB, (c) s-LiBOB, (d) c-LiBOB.

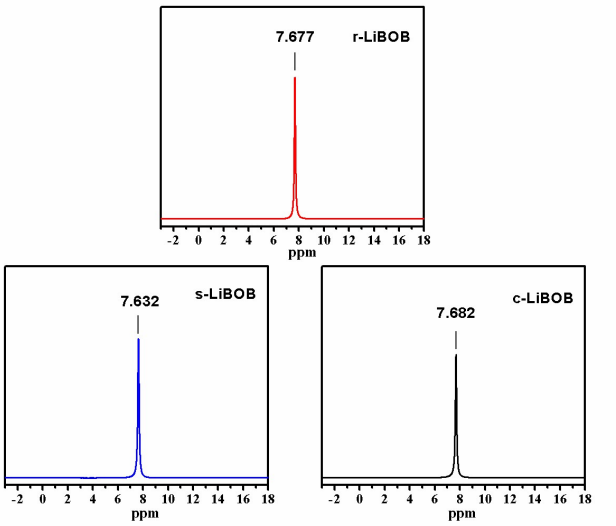

Fig. 2 ^{11}B NMR spectra from: (a) r-LiBOB, (b) pure s-LiBOB, (c) c-LiBOB.

3.2 Mitigating voltage fade of Li-rich cathode by LiBOB as electrolyte additive

The electrochemical performances of $Li_{1.16}[Mn_{0.75}Ni_{0.25}]_{0.84}O_2$ cathode were evaluated in the electrolyte system with and without LiBOB prepared via the rheological phase reaction method. The initial charge/discharge profiles in Fig. 3a appear to be similar, revealing that LiBOB as additive has not altered the lithium intercalation/de-intercalation behavior. The charging voltage slope below 4.5 V is attributed to Li^+ deintercalation along with the oxidation of Ni^{2+} to Ni^{3+} and then to Ni^{4+}, and the voltage plateau above 4.5 V is assigned to the activation of Li_2MnO_3 component accompanied with the irreversible removal of Li_2O. After activation of the Li_2MO_3

component, the cathode material can deliver a high capacity in the subsequent cycles. During the discharge process, the reduction of Ni^{4+} to Ni^{2+} occurs before 3.5V, and the reaction in the low voltage region (< 3.5V) can be attributed to the reduction of Mn^{4+} to Mn^{3+}.[22, 23] The capacity and coulombic efficiency of the initial cycle at the current rate of 0.5C have been listed in Table 1. It can be seen that the initial irreversible capacity (C_{irr}) of the cell slightly increases with an increase of LiBOB content, in detail, the cells with 0.03 M and 0.05 M LiBOB show a little bit larger initial C_{irr} than the one cycled in the pristine electrolyte, which could be ascribed to the formation of LiBOB-involved SEI layer.

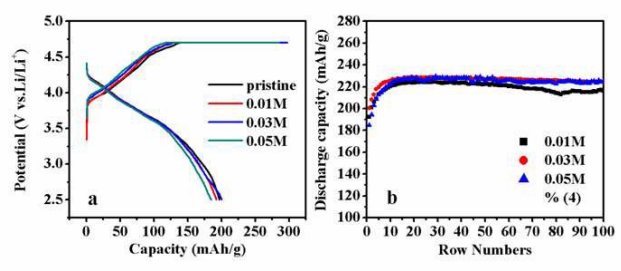

Fig. 3 Charge/discharge characteristics of Li/$Li_{1.16}[Mn_{0.75}Ni_{0.25}]_{0.84}O_2$ cells cycled in the electrolytes with and without LiBOB at 25°C, 2.5-4.7V, 0.5C: (a) charge/discharge profiles of the 1st, (b) cycling performance.

Table 1 The initial cycle data of Li/ $Li_{1.16}[Mn_{0.75}Ni_{0.25}]_{0.84}O_2$ cells in the pristine and electrolytes with various contents of LiBOB: at 25°C, 2.5-4.7V, 0.5C.

Amount of LiBOB (mol/L)	First charge capacity (mAh/g)	First discharge capacity (mAh/g)	C_{irr} (mAh/g)	Coulombic efficiency (%)
0	293.6	196.8	96.8	67.0
0.01	284.9	192.2	92.7	67.5
0.03	297.7	200.2	97.5	67.3
0.05	285.2	184.8	100.4	64.8

The cycling performance in Fig. 3b demonstrates that $Li_{1.16}[Mn_{0.75}Ni_{0.25}]_{0.84}O_2$ material cycled in the pristine electrolyte displays fast capacity degradation during cycling, the discharge capacity decreases to 196.4mAh/g after 100 cycles at 0.5C with capacity retention of 88%; while the ones cycled in the electrolytes with LiBOB show the improved cycling stability, discharge capacities of the cells after 100 cycles with 0.01M, 0.03M and 0.05M LiBOB are 216.4mAh/g, 224.2mAh/g and 225.4mAh/g, corresponding to capacity retention of 96.52%, 97.95% and 98.64% (versus the maximum discharge capacity), respectively. In addition, $Li_{1.16}[Mn_{0.75}Ni_{0.25}]_{0.84}O_2$ shows the increasing discharge capacity concentrated in the 3.5–3.0 V range during the early cycles, i.e., the discharge capacities delivered between 3.5V and 3.0V increase from 52, 45, 45 and 41.6 mAh/g initially to 80.1, 76.7, 78.3 and 69.9 mAh/g of the 10th cycle for the cathode cycled in the pristine electrolyte and with 0.01M, 0.03M and 0.05M LiBOB, respectively. The phenomenon is attributed to the rearrangement of transition metal ions in the delithiated host structure, which make up for the structural deficiencies of the cathode material possibly derived from preparation process such as one-step calcination.

Fig. 4a-d show the evolution for charge/discharge profiles of $Li_{1.16}[Mn_{0.75}Ni_{0.25}]_{0.84}O_2$ cathode in electrolytes with and without LiBOB additive. The cell with the pristine electrolyte shows severe discharge voltage fade upon cycling in Fig. 4a. As the LiBOB content increases from 0.01M to 0.05M, the value of voltage fade during cycling decreases monotonously (Fig. 4b-d). Moreover, detailed comparison of median discharge voltage for different electrolyte system is shown in Fig. 4e. After 60 cycles the material in electrolytes with 0.03M and 0.05M LiBOB exhibits the apparently suppressed growth in median discharge voltage fade as compared with the material cycled in pristine electrolyte and the system with 0.01M LiBOB. Fig. 4f shows the energy density calculated through C×V of the $Li_{1.16}[Mn_{0.75}Ni_{0.25}]_{0.84}O_2$ electrodes, where C is the discharge specific capacity and V is the median discharge voltage. The value of energy density for the cell with pristine electrolyte exhibits a fast decrease after 100 cycles to 630.2Wh/kg with energy retention of 79.81% (versus the maximum energy density), while the cells after 100 cycles with 0.01M, 0.03M and 0.05M LiBOB retain the energy density of 691.6Wh/kg, 724.5Wh/kg and 732.8Wh/kg, corresponding to 87.98%, 90.84% and 92.32%, respectively. The results indicate that the energy degradation of Li-rich electrodes is mitigated significantly with LiBOB as electrolyte additive. In order to further analysis, discharge capacity of $Li_{1.16}[Mn_{0.75}Ni_{0.25}]_{0.84}O_2$ cathode above and below 3.5 V during cycling is displayed in Fig. 5. A decrease on the capacity delivered above 3.5 V (Fig. 5a) and a simultaneous increase on the capacity below 3.5V after 10 cycles (Fig. 5b) for the electrodes reflect the gradual phase transformation of the material during cycling. Generally, there are two main reasons contributing to voltage fade of lithium-rich cathode materials during cycling: one is the deterioration of the electrode/electrolyte interface associated with the parasitic side reactions between electrode and electrolyte at high voltages; the other can be attributed to the structural evolution from layered to spinel-like phase occurs at the surface of the particles and evolves gradually in the internal structure during cycling.[24, 25] As shown in Fig. 5a, the cathode cycled in electrolytes with 0.03M and 0.05M LiBOB exhibits significantly reduced capacity decay above 3.5 V, indicating a suppression of phase transformation.[25] The results indicate that the phase transformation of Li-rich material can be suppressed obviously, but could not be totally avoided in the presence of LiBOB as electrolyte additive. Interestingly, the capacity drop at >3.5 V region is compensated by the capacity increase at <3.5 V region, so the cells with LiBOB additive exhibit an excellent capacity stability. However, the undetectable change in voltage fade of the material with 0.01M LiBOB appears by compared with the one in pristine electrolyte. The fact indicates that the content of 0.01M is too small to create a desirable SEI layer, while 0.03M and 0.05M

LiBOB as electrolyte additive are more appropriate to improve the performances of $Li_{1.16}[Mn_{0.75}Ni_{0.25}]_{0.84}O_2$. It is deduced that LiBOB additive may decompose to form a stable SEI layer which inhibits the deterioration of the electrode/electrolyte interface and also mitigates structural degradation of the active material.

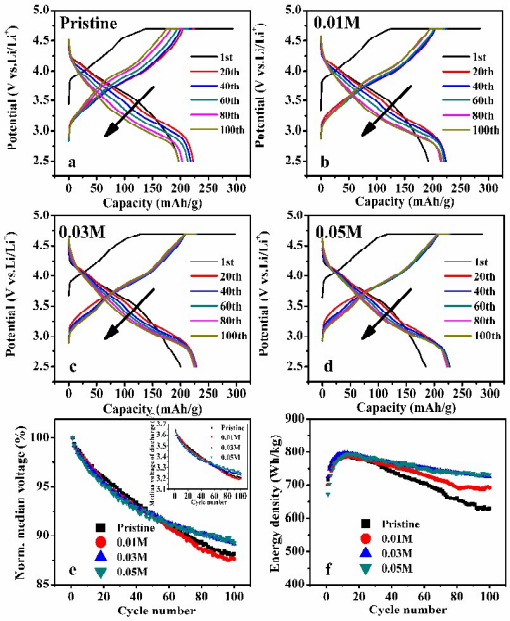

Fig. 4 Charge/discharge profile evolutions of $Li/Li_{1.16}[Mn_{0.75}Ni_{0.25}]_{0.84}O_2$ cells cycled in (a) pristine electrolyte and electrolytes with (b) 0.01M (c) 0.03M (d) 0.05M LiBOB; (e) normalized median discharge voltage and (f) energy density of the cells with and without LiBOB. The inset shows the corresponding median discharge voltage.

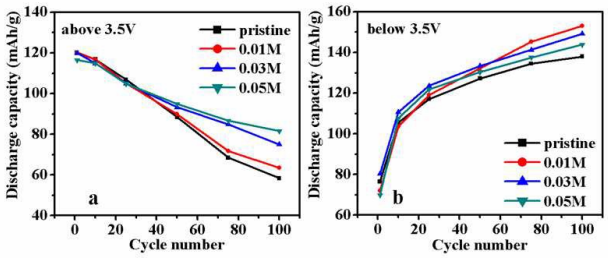

Fig. 5 Discharge capacity (a) above and (b) below 3.5 V during cycling of $Li/Li_{1.16}[Mn_{0.75}Ni_{0.25}]_{0.84}O_2$ cells cycled in the electrolytes with and without LiBOB at 25°C, 2.5-4.7V, 0.5C.

3.3 Effect of LiBOB additive on electrolyte/Li-rich cathode interface

In order to get insight of the functional mechanism of LiBOB additive on mitigating voltage fade of $Li_{1.16}[Mn_{0.75}Ni_{0.25}]_{0.84}O_2$ cathode, CV tests were performed to compare the oxidation potential of electrolytes as shown in Fig. 6. As known, some electrolyte additives preferentially decompose during the initial cycle in order to form a stable electrode/electrolyte interface, which occurs prior to the decomposition of the electrolyte solvents, and thereby guarantees the stability of electrolyte and electrodes.[26, 27] Fig. 6d exhibits the magnification of CV curves for the cells cycled in electrolytes with and without LiBOB additive. An oxidation peak appears at ~4.3 V (vs. Li/Li^+) for the cell with LiBOB additive in the initial charge, which becomes more obvious with an increase of additive content. And the peak almost disappears in the subsequent cycle, indicating the additive oxidation mainly occurs in the first cycle. The results suggest that LiBOB additive does sacrificially decompose on the cathode surface involving in the formation of SEI layer, which inhibits the side reactions on the interface even at high voltage.

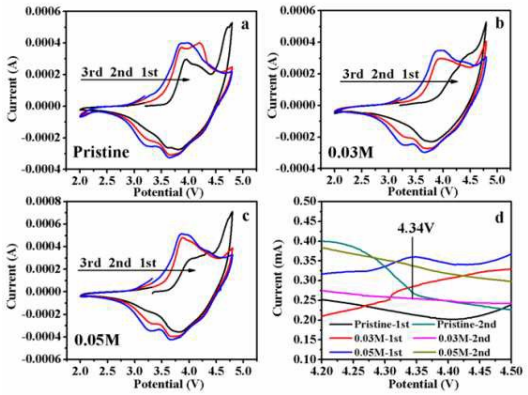

Fig. 6 Cyclic voltammetry (CV) curves of $Li_{1.16}[Mn_{0.75}Ni_{0.25}]_{0.84}O_2$ cycled in (a) pristine electrolyte and electrolytes with (b) 0.03M and (c) 0.05M LiBOB at 25°C, 2.0-4.8V, 0.1mV/s rate, (d) magnification CV curves of the 1st and 2nd cycles for the three types of electrolytes at 4.2-4.5 V.

EIS measurements of $Li/Li_{1.16}[Mn_{0.75}Ni_{0.25}]_{0.84}O_2$ cells were carried out to further evaluate the electrode/electrolyte interfacial behavior. The cells for EIS measurement firstly underwent specific cycles between 2.5-4.7 V at 1C rate and then charged to 4.0 V at 0.2C rate. As shown in Fig. 7, all the Nyquist plots of the cells with and without LiBOB include two semicircles in the frequency region. The semicircle in the high frequency (R_f) is associated with Li^+ migration through the SEI layer on the cathode surface, and the medium-frequency semicircle is attributed to the charge-transfer reaction through the electrode/electrolyte interface (R_{ct}). The values of R_f and Rct were determined by fitting the EIS spectra using the equivalent circuit (Scheme 2[16]), where Rs represents the solution resistance, R_f and CPE_f stand for the resistance and capacitance of SEI layer, R_{ct} and CPE_{dl} correspond to the charge-transfer resistance and double layer capacitance, respectively. The obtained data were summarized in Fig. 8. It can be seen that R_f of the cells without LiBOB decreases from 28.6Ω of the 15th cycle to 21.8Ω of the 30th cycle, and then increases to 30.1Ω of the 50th cycle, especially at 100th cycle surges to 104.1Ω. The dramatic growth of R_f implies that a

thick and less conductive SEI layer forms on the cathode surface in 100 cycles for the cells with the pristine electrolyte. By contrast, the cells with 0.01M and 0.03M LiBOB exhibit small variations in R_f over 100 cycles, which indicates that the LiBOB-involved SEI layer is more stable and effectively suppresses the continuous decomposition of electrolyte on the cathode surface. Although all cells show an increase of R_{ct} upon cycling, the cell with LiBOB exhibits much lower increase in R_{ct} than the ones without LiBOB, which demonstrates that SEI layer derived from LiBOB protects the active material from severe structural degradation. The results confirm that LiBOB has intervened in the electrolyte/cathode interfacial behavior, and thereby suppresses the cell polarization and mitigates the voltage fade of Li-rich cathode.

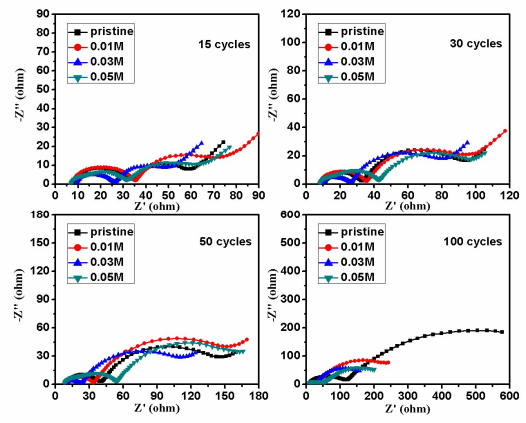

Fig. 7 EIS spectra of 50% DOC $Li_{1.16}[Mn_{0.75}Ni_{0.25}]_{0.84}O_2$ cells without LiBOB and with 0.01M, 0.03M and 0.05M LiBOB at 25°C after (a) 15 cycles, (b) 30 cycles, (c) 50 cycles and (d) 100cycles.

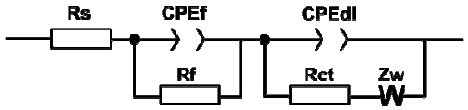

Scheme 2 The equivalent circuit model for EIS data fitting

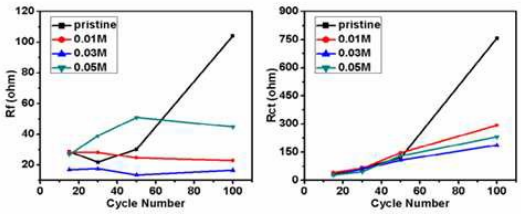

Fig. 8 The fitting results of (a) R_f and (b) R_{ct} from EIS spectra.

XPS spectra of C1s and F1s were carried out to study the surface composition of $Li_{1.16}[Mn_{0.75}Ni_{0.25}]_{0.84}O_2$ cathode cycled in different electrolytes at a current density of 100mA/g after 100 cycles. As displayed in Fig. 9, all C1s spectra are contributed to the absorbed carbon from the atmosphere (284.8 eV) and residual PVDF (C-F at 291.3 eV) on the surface of $Li_{1.16}[Mn_{0.75}Ni_{0.25}]_{0.84}O_2$ cathode. The peaks at 289.3 eV (C=O) and 286.2 eV (C-O)[28] may be attributed to the species with C–O and O–C=O groups such as polyethylene carbonate (PEO), lithium alkyl carbonates (LiOR, $ROCO_2Li$) and oxalates. Moreover, the system with 0.03M LiBOB shows the higher intensity of C=O and C-O peaks than the one cycled in the pristine electrolyte, which may be derived from the decomposition products of LiBOB. The F1s spectrum corresponding only one peak at 688eV for the fresh cathode is ascribed to PVDF.[29] While, the peak at 685.6eV appears in the cathode cycled with and without LiBOB, which demonstrates the presence of LiF associated with the decomposition of $LiPF_6$.[29] It is worthy to note that the intensity of LiF peak reduces obviously in the system with 0.03M LiBOB, which results in a conductive SEI layer as EIS measurements shown.

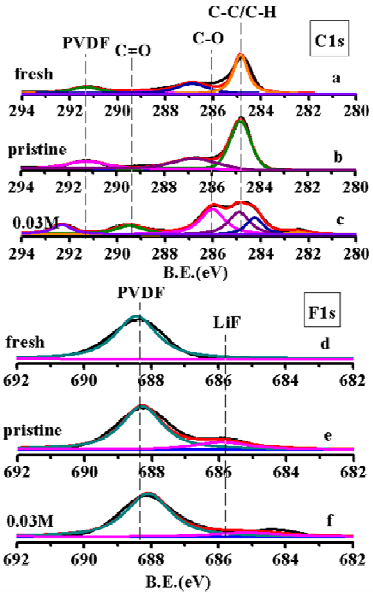

Fig. 9 C1s (a, b, c) and F1s (d, e, f) XPS spectra of fresh $Li_{1.16}[Mn_{0.75}Ni_{0.25}]_{0.84}O_2$ electrode and electrodes cycled in pristine electrolyte and electrolyte with 0.03M LiBOB at 0.5C after 100 cycles.

It is widely accepted that SEI formed on the cathode surface in the $LiPF_6$-EC-based electrolyte consists of inorganic species (LiF, Li_2CO_3, $Li_xPO_yF_z$, Li_xPF_y) as the matrix of SEI layer and organic species (PEO, LiOR and $ROCO_2Li$), which determines the elasticity and flexibility characters of SEI.[30, 31] It can be seen from the results that the SEI film in the cells with LiBOB contains a much larger amount of organic substance and less LiF content. In conclusion of the experimental results, the functional mechanism of LiBOB is proposed as shown in Fig. 10. BOB anion may follow a 1-electron oxidation process to eliminate CO_2 and generate borate radical, which performs the radical coupling reaction to form cross-linking compounds on the cathode surface.[32] The LiBOB-derived SEI layer provides

the stable interface between the electrolyte and the electrode material, where Li^+ diffusion is also facilitated. Although the oxygen release during activation process of the Li_2MnO_3 component at high voltage, the LiBOB-derived SEI layer could minimize the reaction between electrolyte components and the evolved oxygen species, such as superoxide anion O_2^-, and thus decrease the oxidation of electrolyte. Additionally, the acidic species from the electrolyte decomposition may lead to the corrosion of the cathode form the surface to bulk. It is found that the content of acidic species on the surface is also reduced by the LiBOB-derived SEI layer, which suppresses degradation of the cathode structure.[33, 34]

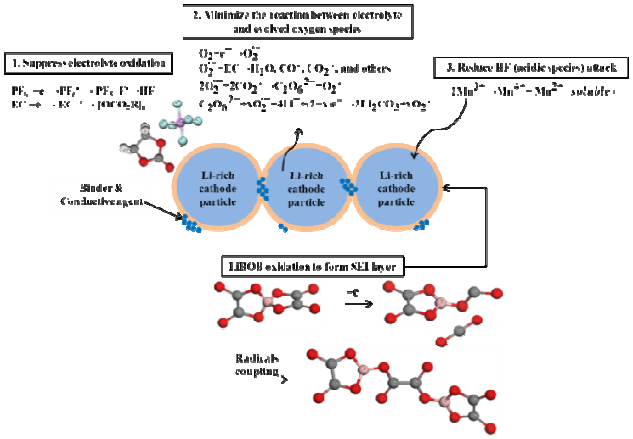

Fig. 10 The possible decomposition process of LiBOB and functions of LiBOB-derived SEI layer.

4. Conclusions

The novel rheological phase reaction method is employed to synthesize lithium salt LiBOB without purification procedure. The results of XRD, ICP, and ^{11}B NMR indicate that the as-obtained LiBOB has high purity comparable to the commercial samples and the one prepared from solid state reaction method with purification. The rheological phase reaction method realizes simplification of the synthetic process for pure LiBOB. Furthermore, LiBOB as electrolyte additive in $Li_{1.16}[Mn_{0.75}Ni_{0.25}]_{0.84}O_2$ cells has been investigated herein. The results confirm that LiBOB additive participates in the reaction for SEI film formation, which improves the interfacial stability and mitigates the structural deterioration of lithium-rich cathode. The issues in discharge voltage fade and energy degradation can also be eased in presence of LiBOB as electrolyte additive.

Acknowledgements

This work was financially supported by the National 863 Program of China (No.2013AA050901).

References

1 J. L. Allen, S.-D. Han, P. D. Boyle and W. A. Henderson, *J. Power Sources*, 2011, **196**, 9737-9742.
2 Z. Ma, T. Li, Y. L. Huang, J. Liu, Y. Zhou and D. Xue, *RSC Adv.*, 2013, **3**, 7398-7402.
3 M. Armand and J. M. Tarascon, *Nature*, 2008, **451**, 652-657.
4 S. Li, Y. Zhao, X. Shi, B. Li, X. Xu, W. Zhao and X. Cui, *Electrochim. Acta*, 2012, **65**, 221-227.
5 K. Xu, *Chem. Rev.*, 2004, **104**, 4303-4417.
6 V. Aravindan, J. Gnanaraj, S. Madhavi and H.-K. Liu, *Chem. Eur. J.*, 2011, **17**, 14326-14346.
7 J.-C. Panitz, U. Wietelmann, M. Wachtler, S. Ströbele and M. Wohlfahrt-Mehrens, *J. Power Sources*, 2006, **153**, 396-401.
8 W. Xu and C. A. Angell, *Electrochem. Solid-State Lett.*, 2001, **4**, E1-E4.
9 K. Xu, S. S. Zhang, U. Lee, J. L. Allen and T. R. Jow, *J. Power Sources*, 2005, **146**, 79-85.
10 S.-T. Myung, H. Natsui, Y.-K. Sun and H. Yashiro, *J. Power Sources*, 2010, **195**, 8297-8301.
11 B.-T. Yu, W.-H. Qiu, F.-S. Li and G.-X. Xu, *Electrochem. Solid-State Lett.*, 2006, **9**, A1-A4.
12 K. Xu, *J. Electrochem. Soc.*, 2008, **155**, A733-A738.
13 X. Wu, S. Wang, X. Lin, G. Zhong, Z. Gong and Y. Yang, *J. Mater. Chem. A*, 2014, **2**, 1006-1013.
14 G. Xu, Z. Liu, C. Zhang, G. Cui and L. Chen, *J. Mater. Chem. A*, 2015, **3**, 4092-4123.
15 S. S. Zhang, *J. Power Sources*, 2006, **162**, 1379-1394.
16 M. Gao, F. Lian, H. Liu, C. Tian, L. Ma and W. Yang, *Electrochim. Acta*, 2013, **95**, 87-94.
17 Y. Li, F. Lian, L. Ma, C. Liu, L. Yang, X. Sun and K. Chou, *Electrochim. Acta*, 2015, **168**, 261-270.
18 S. J. Lee, J. G. Han, I. Park, J. Song, J. Cho, J. S. Kim and N. S. Choi, *J. Electrochem. Soc.*, 2014, **161**, A2012-A2019.
19 P. Y. Zavalij, S. Yang and M. S. Whittingham, *Acta Cryst.*, 2003, **B59**, 753-759.
20 S. Wang, W. Qiu, T. Li, B. Yu and H. Zhao, *Int. J. Electrochem. Sci.*, 2006, **1**, 250-257.
21 U. Wietelmann, U. Lischka and M. Wegner, *U.S. Pat.*, 6 506 516, 2003.
22 S. Rajarathinam, S. Mitra and R. K. Petla, *Electrochim. Acta*, 2013, **108**, 135-144.
23 S. Park, S. Kang, C. Johnson, K. Amine and M. Thackeray, *Electrochem. Commun.*, 2007, **9**, 262-268.
24 J. Zheng, M. Gu, A. Genc, J. Xiao, P. Xu, X. Chen, Z. Zhu, W. Zhao, L. Pullan, C. Wang and J. G. Zhang, *Nano Lett.*, 2014, **14**, 2628-2635.
25 J. Zheng, M. Gu, J. Xiao, B. J. Polzin, P. Yan, X. Chen, C. Wang and J. Zhang, *Chem. Mater.*, 2014, **26**, 6320-6327.
26 J. Zhang, J. Wang, J. Yang and Y. NuLi, *Electrochim. Acta*, 2014, **117**, 99-104.
27 S. Tan, Z. Zhang, Y. Li, J. Zheng, Z. Zhou and Y. Yang, *J. Electrochem. Soc.*, 2013, **160**, A285-A292.
28 S. K. Martha, J. Nanda, G. M. Veith and N. J. Dudney, *J. Power Sources*, 2012, **216**, 179-186.
29 L. Liao, X. Cheng, Y. Ma, P. Zuo, W. Fang, G. Yin and Y. Gao, *Electrochim. Acta*, 2013, **87**, 466-472.

30 L. Baggetto, D. Mohanty, R. A. Meisner, C. A. Bridges, C. Daniel, D. L. Wood Iii, N. J. Dudney and G. M. Veith, *RSC Adv.*, 2014, **4**, 23364–23371.
31 Y.-M. Lee, K.-M. Nam, E.-H. Hwang, Y.-G. Kwon, D.-H. Kang, S.-S. Kim and S.-W. Song, *J. Phys. Chem. C*, 2014, **118**, 10631-10639.
32 M. Xu, N. Tsiouvaras, A. Garsuch, H. A. Gasteiger and B. L. Lucht, *J. Phys. Chem. C*, 2014, **118**, 7363-7368.
33 N.-S. Choi, J.-G. Han, S.-Y. Ha, I. Park and C.-K. Back, *RSC Adv.*, 2015, **5**, 2732-2748.
34 J. Zheng, M. Gu, J. Xiao, P. Zuo, C. Wang and J.-G. Zhang, *Nano Lett.*, 2013, **13**, 3824-3830.

High-purity LiBOB, synthesized via novel rheological phase reaction method without further recrystallization, mitigated voltage-fade of Li-rich cathode as electrolyte additive.